

# Advancing hyperspectral CubeSat monitoring with the CSIMBA IOD mission

**Stefan Livens<sup>1</sup>, Bavo Delauré<sup>1</sup>, Dirk Nuyts<sup>1</sup>, Iskander Benhadj<sup>1</sup>, Joris Blommaert<sup>1</sup>,  
Klaas Tack<sup>2</sup>, Roberto Di Paola<sup>3</sup>, Eric Callut<sup>4</sup>, Luca Maresi<sup>5</sup>, Helen Strese<sup>5</sup>, Mikko  
Viitala<sup>6</sup>**

<sup>1</sup>VITO

Boeretang 200, B-2400 Mol, Belgium  
Phone: +32 14 33 68 33, Mail: [stefan.livens@vito.be](mailto:stefan.livens@vito.be)

<sup>2</sup>imec

Kapeldreef 7, B-3001 Leuven, Belgium  
Phone: +32 16 28 14 36, Mail: [klaas.tack@imec.be](mailto:klaas.tack@imec.be)

<sup>3</sup>AMOS

Rue des Chasseurs Ardennais, B-4031 Angleur, Belgium  
Phone: +32 4 361 40 40, Mail: [roberto.dipaola@amos.be](mailto:roberto.dipaola@amos.be)

<sup>4</sup> Deltatec

Rue Gilles Magnée 92/6, B-4430 Ans, Belgium  
Phone: +32 4 239 78 80, Mail: [e.callut@deltatec.be](mailto:e.callut@deltatec.be)

<sup>5</sup> ESA-ESTEC

Keplerlaan 12200 Ag noordwijk, the Netherlands  
Phone: +31 71 565 49 68, Mail: [Luca.Maresi@esa.int](mailto:Luca.Maresi@esa.int)

<sup>6</sup> Aerospacelab SA/NV

Rue André Dumont 9, B-1435 Mont-Saint-Guibert, Belgium,  
Phone: +31 474 52 08 08, Mail: [mikko.viitala@aerospacelab.be](mailto:mikko.viitala@aerospacelab.be)

## Abstract:

We present the CSIMBA project: the development on a hyperspectral instrument for a IOD mission. Its core is a hyperspectral sensor with thin film interference filters directly deposited on a 2D detector. It covers a spectral range of 475nm to 900nm with 5nm spectral resolution. Additional imaging areas allow to perform also panchromatic acquisitions. The instrument also includes a compact wide swath TMA telescope and will be accommodated in a 12u Cubesat platform. Operating from 500km altitude it will provide 20 m GSD and a 80 km swath and. Powerful read out electronics and onboard computing capabilities support advanced acquisition and processing modes. Digital time delay integration (TDI) with up to 12 stages allows a major increase in SNR. Dedicated imaging modes optimize imaging for higher dynamic range and very low signals. The combined use of panchromatic and hyperspectral imaging is also explored, aiming at increased spatial detail through computational imaging techniques. Performance analysis using simulations on realistic spectra show that results with useful quality can be obtained. This fits with the overall goal to provide enhanced vegetation monitoring of agricultural fields and the biodiversity status, with short revisit rates when a constellation is put in place.

# 1. INTRODUCTION

## 1.1 Small hyperspectral missions

Remote sensing is the tool of choice to transform the bio-economy into a more efficient and sustainable industry, ready to face major global challenges. The entire value chain from seed/plant breeders, seed/plant multipliers, operational & commercial farming to food processing industry can benefit hugely from objective measurements enabled by remote sensing solutions. Large scale operational monitoring with short revisit times, necessary to achieve the benefits, is best organized by using satellite platforms. Using hyperspectral imagers for monitoring can maximize its benefits because the detailed spectral information can reveal crucial information on the condition of vegetation faster and more accurately.

In the past hyperspectral imaging from satellite platforms was limited to exploratory scientific experiments. A few specialized missions carrying complex instruments (like Hyperion onboard EO-1 and CHRIS on PROBA [1,2]) were able to image only confined areas very infrequently because of limited data downlink and detector capabilities. Currently, besides the continued efforts to develop high-end hyperspectral missions, including EnMAP and PRISMA [3,4], there is also a trend towards smaller and more agile hyperspectral missions.

Recently, technological progress has allowed to develop and launch much more compact and lighter hyperspectral instruments and missions. Some of the most radically innovative designs use narrow-band thin film interference filters. They are able to collect full spectral images and demonstrate capabilities which until recently were only possible with much larger instruments and platforms. An early example is the Hyperscout mission [5], a small Cubesat mission which uses a frame sensor with a linear variable filter. Initial results from such missions show that they manage to achieve some ambitious goals. Still, challenges like platform stability, data downlink limitations and lower image quality hinder the adoption of their data for many applications.

## 1.1 CSIMBA

The CSIMBA project (Compact Smartspectral Imager for Monitoring Bio-agricultural Areas) aims to push the technology significantly by developing a proto-flight model compact hyperspectral instrument which is suitable to use in an in orbit demonstration mission. The CSIMBA focuses on improving image quality to a level where it is sufficient to enable demanding applications relying on precise narrowband spectral information.

The rationale behind this is found in the most promising use case for such small missions: providing data not covered by the main missions. Since similar spatial and spectral characteristics are or will become available, providing data at different points in time will be most useful. However, the small mission data can only be introduced in time series of high-end missions if the quality is sufficient [6].

## 2. INSTRUMENT DEVELOPMENT

### 2.1 Acquisition principle

We make use of a “pushframe camera”. It uses a frame sensor which has spectral filters arranged in a line-wise fashion on the sensor. It uses narrow-band filters arranged in a line-wise pattern on the sensor. Full hyperspectral information is built up by capturing images in rapid succession while scanning over an area, as illustrated in *Figure 1*. This makes it operationally similar to a pushbroom camera, making it ideally suited for use onboard satellite systems. The individual acquisitions however have the advantage that each frame contains a meaningful 2D view of the area which allows to generate very precise spatial registration. At the same time, the pushframe principle has much better light collecting properties than both frame based images and pushbroom systems. [7]

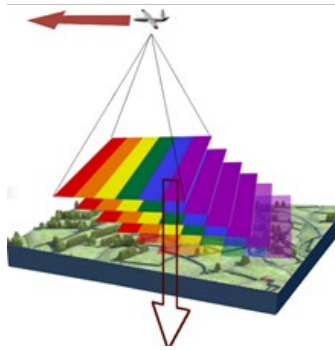


*Figure 1 Illustration of the scanning to build up a spectral hypercube.*

### 2.2 Compact Hyperspectral Imaging engineering Model (CHIEM)

CSIMBA capitalizes upon our earlier developments, most importantly the ESA-GSTP project CHIEM in which an engineering model hyperspectral camera was developed making use of a sensor with direct filter deposition [8]. The direct on sensor filter deposition, developed by imec, greatly outperforms systems using classical linear variable filters because it allows pixel-precise control of the spectral response and thus also allowing to have several sensor lines with the same spectral filter, increasing the sensitivity.

Sensors based on this technology have been developed earlier, they have been successfully used to build hyperspectral RPAS cameras [9]. They provide a very useful spectral range of 475 to 900 nm with a spectral resolution (FWHM) of about 5 nm. With CHIEM the spectral range was retained, but using a larger CMOS sensor with 12Mpx instead of 2Mpx, both higher spatial resolution and a wider swath could be obtained. Also, more detector lines (12 instead of 5 or 8) per spectral band can be used. The sensor also accommodate two panchromatic zones. The layout of the sensor chip is shown in *Figure 2*.

### 2.2 Read out electronics (ROE)

The sensor is accompanied by a very powerful custom designed ROE unit. Its main discerning feature is that it supports very high data rates. To get full spectral coverage of an area, the mission parameters dictate that images are acquired continuously with a speed of at least 30 fps. The ROE however supports much faster readout, in fact 12x faster for the full hyperspectral area.

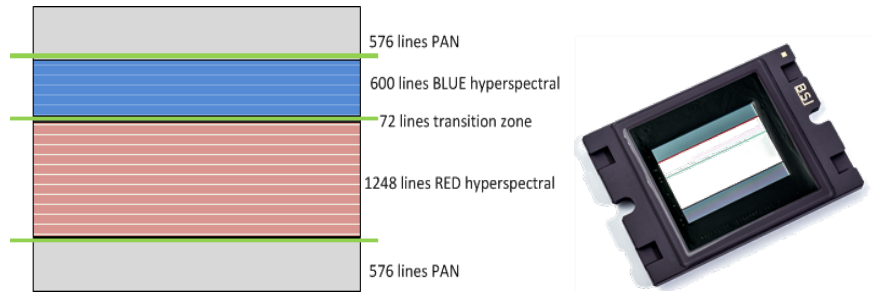


*Figure 2 left: Layout of the CHIEM sensor, right: photo of the sensor.*

Facilities have been foreseen to perform digital accumulation of the incoming data, which in fact implements a digital version of Time Delay integration (TDI) with up to 12 stages. It also allows to enable high dynamic range imaging. Additional facilities allow pre-processing of the data including photo response non-uniformity corrections and, and bad pixel replacement. The onboard computing power will also be put into action to reduce the data amount prior to the transmission to ground.

To make the ROE work well in a space environment, a hybrid design philosophy has been employed, in which smart choices have been made by including both radiation hard components as well as COTS components, and by implementing fault tolerant mechanisms. The physical layout of the ROE unit is shown in *Figure 3*.

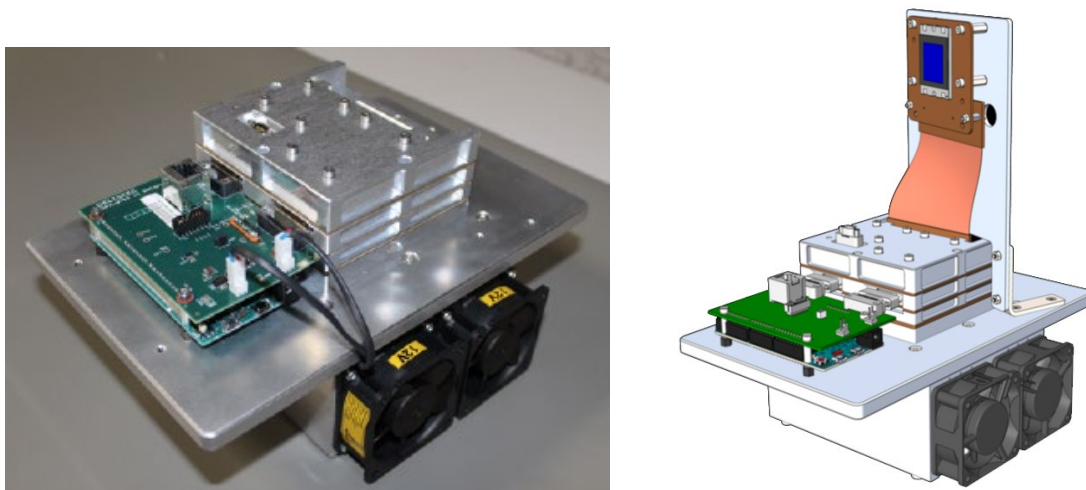


*Figure 3 Read-out electronics with sensor*

### 3.2 Optics and instrument layout

A custom compact Three Mirror Anastigmat (TMA) telescope has been designed for the CSIMBA instrument by project partner AMOS. It is suitable to fit into a 12U CubeSat platform and optimized for the size of the sensor as well as. The TMA has a large Field-of-view (across track:  $\pm 4.75$  deg, along track 3.6 deg with minor vignetting). It has an F number of  $f/4.5$  and a focal length of 135mm to enable the CSIMBA GSD of 20m. The layout of the instrument is shown in *Figure 4*, containing the TMA, the ROE and the hyperspectral focal plane.

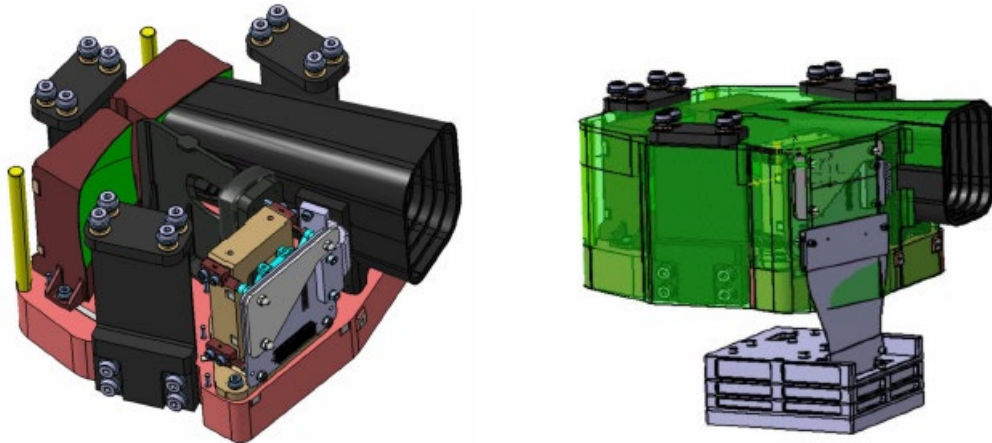


*Figure 4 CSIMBA instrument consisting of a Three Mirror Anastigmat, sensor and ROE*

The design meets all the image quality criteria as set for the CSIMBA mission. The instrument is able to sustain flight environmental conditions (vibrations, temperature variations) and the sustainable shock levels have been analysed. The athermality of the full aluminium design has been validated through opto-thermal analyses. Compliance is achieved for each requirement. This confirms the maturity of the design, which is ready for manufacturing.

### **3.3 Platform and downlink**

The platform has been designed which can accommodate all components inside a 12U CubeSat frame. It is shown in Figure 5. Mass and power budgets have been detailed. The result is that the 12U platform is feasible and suitable for a demonstration of the CSIMBA PFM instrument.

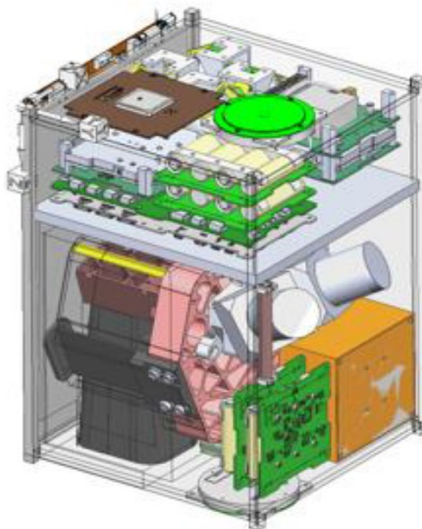


**Figure 5 CSIMBA instrument integrated in a 12U CubeSat**

It has several limitations towards an operational mission. The available space does not allow to add facilities for propulsion, so no manoeuvring capability would be possible in a constellation implementation. The available power is also limited, which in turn limits the data downlink capacity, and thus the total imaging which can be realized per day. The

theoretical downlink capacity is 50Mb/s, which with some margin and room for telemetry data reduces to 38.6 Mb/s, with total downlink time is about 8 minutes.

### 3. CSIMBA INSTRUMENT PERFORMANCE

#### 3.1 Imaging sharpness

We investigate the sharpness and level of detail which can be imaged and express those in term of the modulation transfer function MTF. We define the system MTF as the product of the diverse contributing elements:

$$MTF_{system} = MTF_{sensor} \times MTF_{optics} \times MTF_{lin.motion} \times MTF_{rand.motion} \times MTF_{TDI} \times MTF_{atm.}$$

In which we consider following contributions:

- Instrument MTF: Sensor MTF and Optics MTF
- MTF contribution by linear forward motion
- MTF contribution by random motion
- MTF contribution by TDI process
- Atmosphere MTF caused by turbulence & diffusion

The resulting system MTF curve is shown in Figure 6. The CMV12000 sensor has a pixel size of 5.5um which leads to a Nyquist frequency of 90.91 lp/mm. Unfortunately, the system MTF at Nyquist only equals 0.127, which is lower than the targeted value of 0.2, which is reached around 75 lp/mm.

To mitigate this, several approaches will be considered. A reduction on the number of TDI stages or decrease in integration time would certainly help, albeit at the expense of reducing the SNR. Alternatively, we will investigate to use panchromatic images to increase the sharpness of the hyperspectral band images.

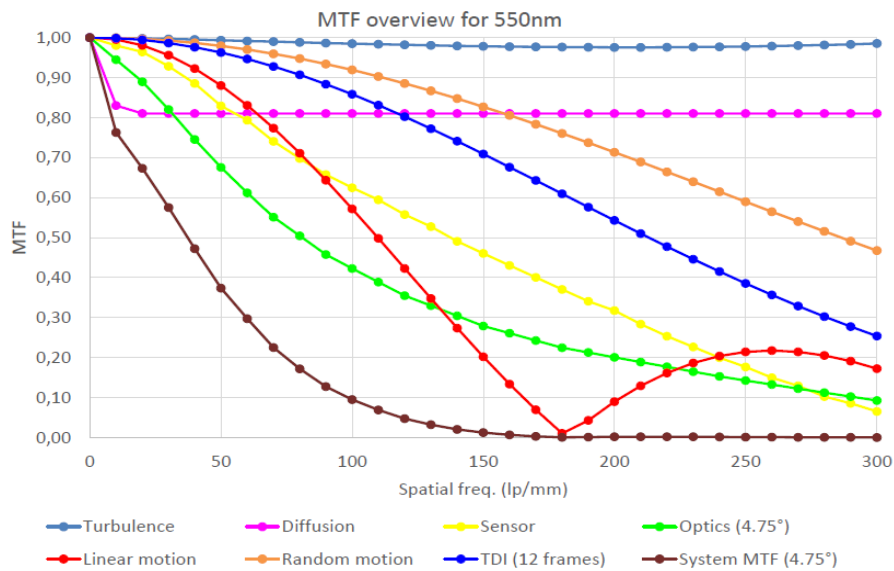


Figure 6: MTF curves for system MTF and its various contributors

### 3.1 Signal to noise ratio

The other basic quantity to describe the quality of the imagery is the signal to noise ratio (SNR). The estimation of this has been made in increasing level of detail.

A first indication of the achievable SNR can be derived from the Full Well Capacity (FWC) of the sensor, which represents the photon shot noise of the sensor, when used with ample light. This gives an upper limit to the achievable SNR from a single acquisition. In reality the spectral bands of the sensor have sensitivities which vary quite strongly. If we take this into account and make sure the sensor does not saturate for the most sensitive bands, all others collect less signal and have lower SNR, leading to spectral SNR curves as shown in Figure 7.

When we assume a flat spectrum of  $100 \text{ W.m}^{-2}.\text{sr}^{-1}.\mu\text{m}^{-1}$  as reference radiance, we find out that even with the maximal integration time, we do collect the maximal amount of light. Beyond shot noise, we also consider other noise sources: read noise, dark noise and quantisation noise. As a result, the SNR is further reduced somewhat, mainly due to the read noise making a contribution esp. for lower signals.

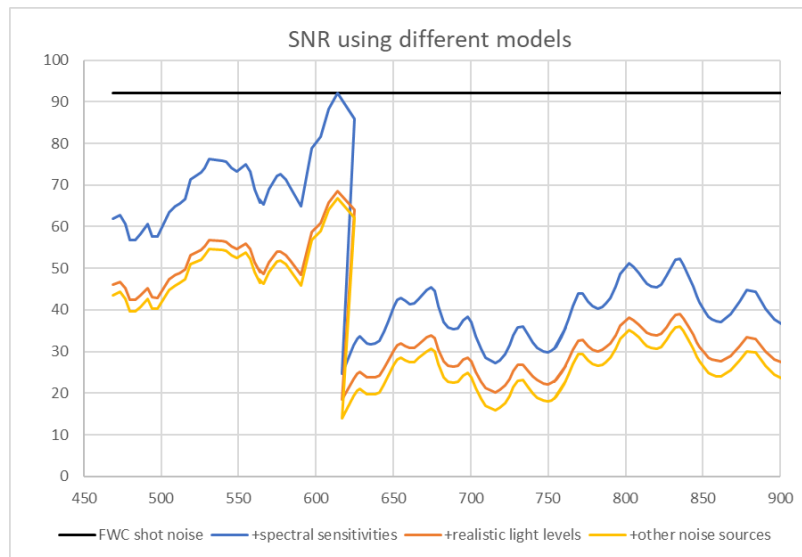


**Figure 7 spectral SNR using various models**

The above clearly illustrates the need to improve the SNR, and thus the importance of the digital TDI capability of the CSIMBA instrument. The TDI step sums up the signal pixel by pixel, which results in an image with higher signal (12 times) and higher SNR ( $\sqrt{12}$ ). The result is shown in Figure 8 (grey curve).

Since the signal itself can take on any spectral shape, we refine the SNR estimates by considering a small set of realistic spectra. We start from typical reflectance spectra (minimum and maximal envelopes, sand and vegetation), and convert them to TOA radiance using atmospheric modelling using a realistic irradiance. Results of SNR estimates on them are shown in the other curves also shown in Figure 8. They show a strong dependence on the wavelength, which may impact the suitability of the data for some applications depending on the importance of specific wavelengths.



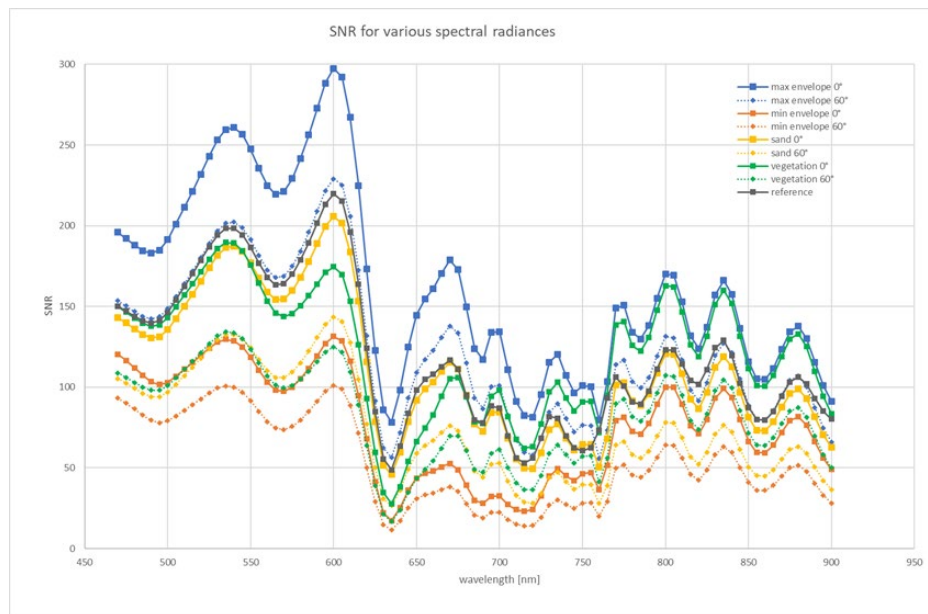


**Figure 8: spectral SNR for realistic spectra, using 12 stage digital TDI**

#### 4. REFERENCES

- [1] M. Marshall, P. Thenkabail, Advantage of hyperspectral EO-1 Hyperion over multispectral IKONOS, GeoEye-1, WorldView-2, Landsat ETM+, and MODIS vegetation indices in crop biomass estimation, ISPRS Journal of Photogrammetry and Remote Sensing, Vol. 108, Pages 205–218, Oct. 2015.
- [2] M. Rast and T. Painter, Earth Observation Imaging Spectroscopy for Terrestrial Systems: An Overview of Its History, Techniques, and Applications of Its Missions, Surveys in Geophysics (2019) 40:303–331
- [3] L. Guanter et al, The EnMAP Spaceborne Imaging Spectroscopy Mission for Earth Observation, Remote Sensing, 7(7), 8830-8857, 2015
- [4] M. Meini, et al, The PRISMA Mission Hyperspectral Payload, Proc. 66th Int. Astronautical Congress (IAC 2015), Jerusalem, Israel, Oct.12-16, 2015.
- [5] M. Soukup et al, HyperScout: Onboard Processing of Hyperspectral Imaging Data on a Nanosatellite, Proc 4S conference, Valletta, Malta, May 2016
- [6] S. Livens : CSIMBA hyperspectral CubeSat in orbit demonstration mission, ESA – ESRIN Workshop on Int. Cooperation in Spaceborne Imaging Spectroscopy, Frascati, Italy, 9 – 11 July 2019
- [7] S. Livens, Comparing hyperspectral imaging concepts using key properties, Proc Whispers 2018, Amsterdam, The Netherlands
- [8] Blommaert, J., Delauré, B., Livens, S., et al. CHIEM: A versatile compact hyperspectral imager in proceedings of the Small Satellites, Systems & Services Symposium – The 4S Symposium 2018
- [9] Sima, A et al., Compact Hyperspectral Imaging System (COSI) For Small Remotely Piloted Aircraft Systems (RPAS) – System Overview and First Performance Evaluation Results, in Int. Arch. Phot. Remote Sens. Spatial Inf. Sci., XLI-B1, 1157-1164, doi:10.5194/isprs-archives-XLI-B1-1157-2016, 2016